**Supporting Information:**

# Buffer Layer Assisted Epitaxial Growth of Perfectly Aligned Oxide Nanorod Arrays in Solution

Gong Ping Li [†], Lin Jiang [‡], Shi Jie Wang [§], Xiao Wei Sun [#], Xiaodong Chen [‡], Tom Wu *[†]

[†] Division of Physics and Applied Physics, School of Physical and Mathematical Sciences, Nanyang Technological University, Singapore 637371 (Singapore), E-mail: tomwu@ntu.edu.sg

[‡] School of Materials Science and Engineering, Nanyang Technological University, Singapore, 639798 (Singapore)

[§] Materials Science and Characterization Cluster, Institute of Materials Research and Engineering, Singapore 117602 (Singapore)

[#] School of Electrical & Electronic Engineering, Nanyang Technological University, Singapore 639798 (Singapore)

1. Additional SEM images of the ZnO NRs synthesized on the $ZnAl_2O_4$ epilayer/ α-sapphire substrates
2. Fitting diameters and heights of NRs as functions of their density
3. SEM images of ZnO NRs grown on the α-sapphire substrates partially covered with a thick $ZnAl_2O_4$ layer
4. Growth behaviors of ZnO NRs on the $ZnAl_2O_4$/ (0001) sapphire (c plane) substrates
5. Vertically aligned ZnO nanoneedles fabricated on the $ZnAl_2O_4$/ α-sapphire substrates
6. Growth behaviors of ZnO NRs on the $MgAl_2O_4$ epilayer/ α-sapphire substrates

## 1. Additional SEM images of the ZnO NRs synthesized on the $ZnAl_2O_4$ epilayer/ α-sapphire substrates

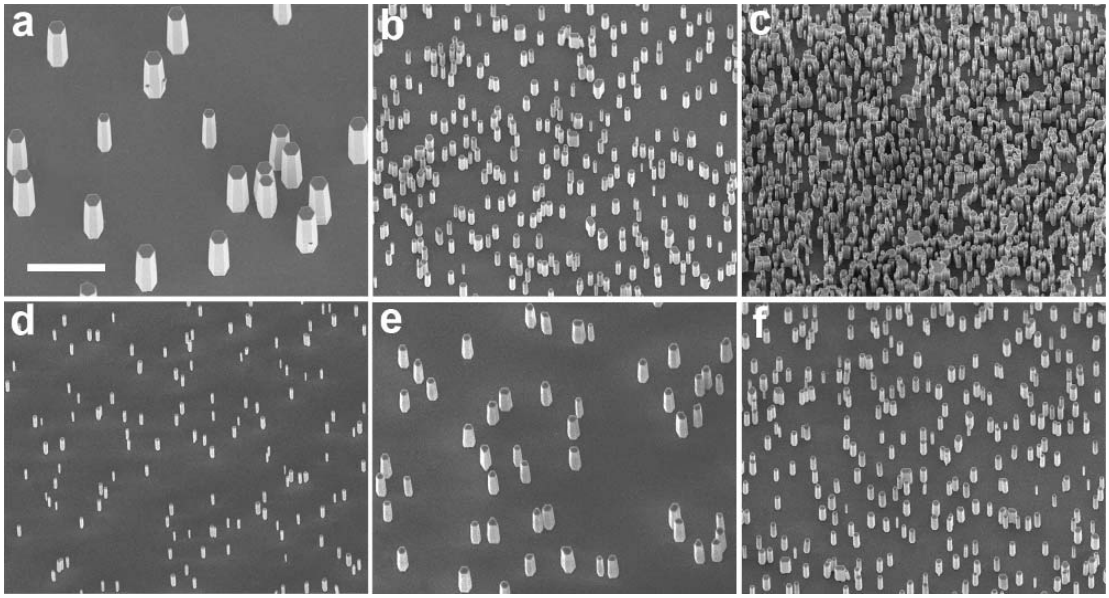


**Figure S1.** SEM images of the ZnO NRs grown on the $ZnAl_2O_4$/α-sapphire substrates which were formed by annealing at (a) 800 °C, (b) 900 °C and (c) 1000 °C, with $[Zn(NO_3)_2]$= 20 mM. SEM images of the ZnO NRs grown on the $ZnAl_2O_4$/α-sapphire substrates which were prepared at 900 °C, with $[Zn(NO_3)_2]$: (d) 5 mM (e) 10 mM and (f) 20 mM. All the figures have the same scale bar of 10 μm.

## 2. Fitting diameters and heights of NRs as functions of their density

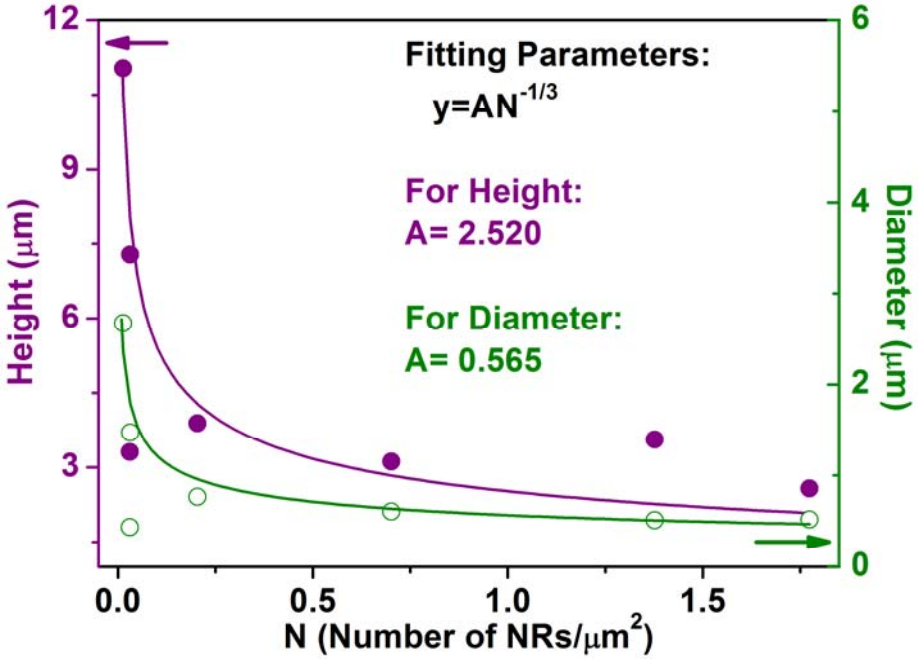


**Figure S2.** Fitting diameters and heights of NRs to a function that $y = \frac{A}{\sqrt[3]{N}}$. The constant A has a dimension of $\mu m^{1/3}$.

## 3. SEM images of ZnO NRs grown on the α-sapphire substrates partially covered with a thick $ZnAl_2O_4$ layer

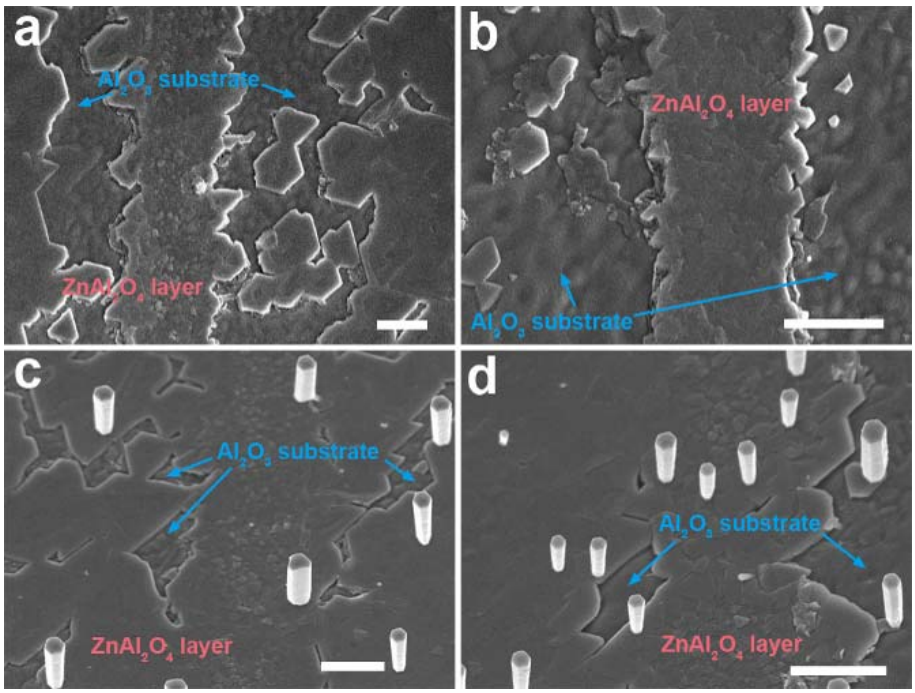


**Figure S3.** SEM images of the $ZnAl_2O_4$ layer on the α-sapphire substrate formed by annealing at 1000 °C before (a, b) and after (c, d) growing the ZnO NRs. The scale bars represent 1 μm. It is clear that the ZnO NRs can only grow on $ZnAl_2O_4$ covered regions, whereas the exposed sapphire surface cannot initiate any NR nucleation.

## 4. Growth behaviors of ZnO NRs on the $ZnAl_2O_4$/ (0001) sapphire (c plane) substrates

For the (0001) sapphire (c plane) substrate, previous studies demonstrated that epitaxial $ZnAl_2O_4$ layer can also be generated if the annealing temperature is higher than 850 °C,[S1, S2] which is consistent with our experiments. From the XRD measurements, we found that $ZnAl_2O_4$ (111), (222) and (333) are the most intense peaks (Figure S4b). However, the presence of other strong $ZnAl_2O_4$ peaks implies a poor epitaxial relationship at the interface. Moreover, the surface rms roughness of the $ZnAl_2O_4$ layer is much larger than that formed on α-sapphire at the same temperature (Figure S4a). These factors result in the NRs grown on the $ZnAl_2O_4$/c-sapphire substrate showing poorer orientation and density controls than the $ZnAl_2O_4$/α-sapphire counterpart (Figure S4c-e).

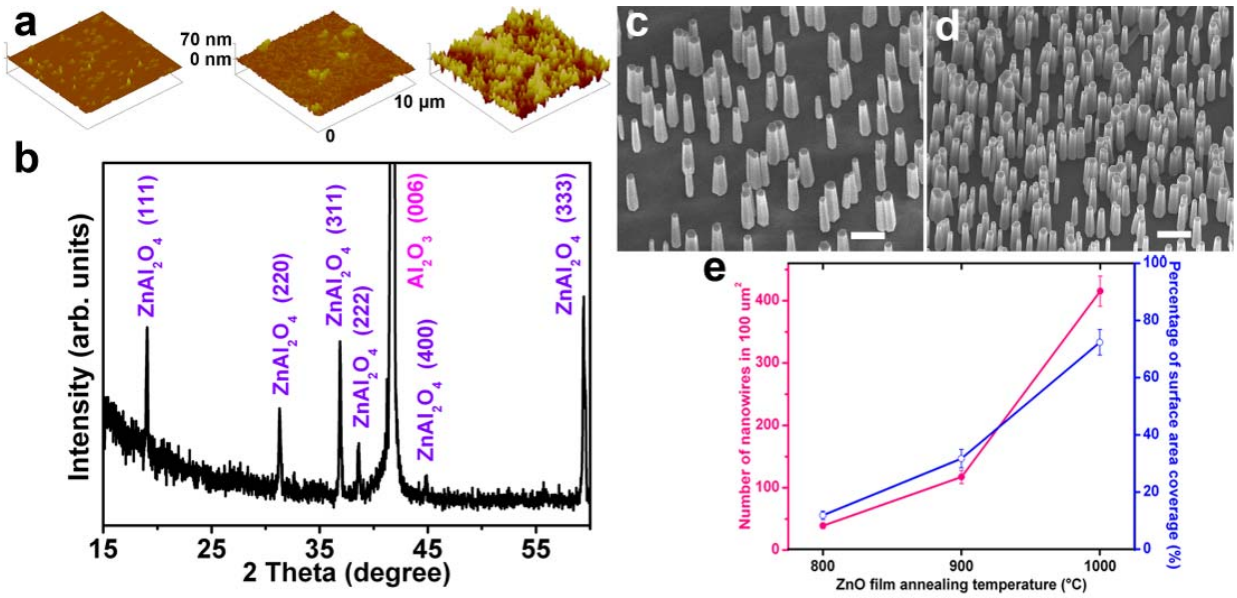


**Figure S4.** (a). AFM micrographs of the $ZnAl_2O_4$/c-sapphire substrates created by annealing at 800, 900 and 1000 °C, the rms roughnesses are 2.415 nm, 4.204 nm, 19.365 nm, respectively. (b). XRD spectra of the $ZnAl_2O_4$/c-sapphire substrate formed at 1000 °C. SEM images of ZnO NRs grown on the $ZnAl_2O_4$/c-sapphire substrates which were created by annealing at (c) 800 °C and (d) 900 °C, $[Zn(NO_3)_2]$= 20 mM. The scale bars represent 2 μm. (e). Dependences of density and surface area coverage on the $ZnAl_2O_4$ forming temperature.

## 5. Vertically aligned ZnO nanoneedles fabricated on the $ZnAl_2O_4$/α-sapphire substrates

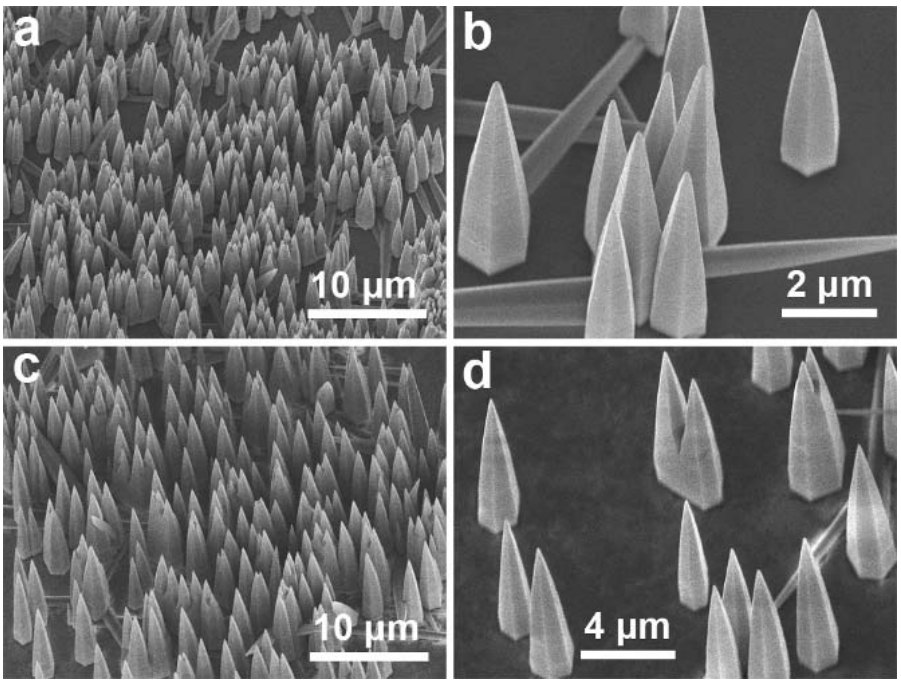


**Figure S5.** Based on previous reports,[S3] we modified the morphology of the ZnO NRs to hexagonal nanoneedles through adding 1, 3-diaminopropane (DAP) into the reactive solution. The ZnO nanoneedles were fabricated on the $ZnAl_2O_4$/α-sapphire substrates which were prepared at 900 °C. [$Zn(NO_3)_2$]= 20 mM, [DAP]: (a, b) 140 mM and (c, d) 160 mM. The nanoneedles have perfect vertical alignment, but in some cases there exits coalescence at their bottom.

## 6. Growth behaviors of ZnO NRs on the $MgAl_2O_4$ epilayer/ α-sapphire substrates

In order to illustrate the generality of our surface engineering protocol on realizing the epitaxial growth of ZnO NRs, we also fabricated $MgAl_2O_4$ epilayers on α-sapphire substrates in order to compare with the $ZnAl_2O_4$ counterpart on assisting the growth of ZnO NRs. MgO layers were first sputtered on the substrates using DC sputtering. After annealing in air at high temperatures (≥800 °C) and subsequent etching in diluted acid to remove the residual MgO, the $MgAl_2O_4$ layers with different roughness were obtained. We found that the magnitude of roughness tunability for $MgAl_2O_4$ layer is much smaller than that of $ZnAl_2O_4$ with the same synthesis parameters, indicating that its modulation for ZnO NR density is less effective than $ZnAl_2O_4$ (Figure S6). Furthermore, the hydrolysis of MgO makes the preparation of clean $MgAl_2O_4$ layers much more difficult. This control experiment further underscores the unique advantages of $ZnAl_2O_4$ as buffers layers to support the growth of high quality ZnO NRs.

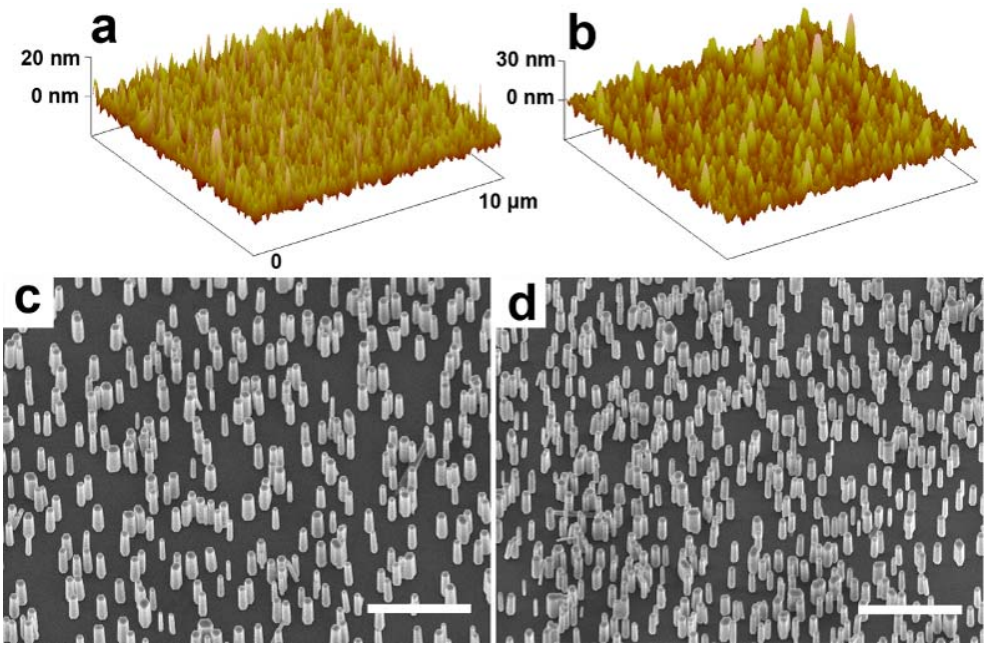


**Figure S6.** AFM micrographs of the $MgAl_2O_4$/α-sapphire substrates produced by annealing at (a) 800 °C and (b) 900 °C, the rms roughnesses are 3.225 nm and 4.024 nm, respectively. (c) and (d) Corresponding SEM images of the ZnO NRs grown on the substrates (a) and (b) at 70 °C with $[Zn(NO_3)_2]$= 20 mM. All the scale bars represent 10 μm.

**REFERENCES:**

(S1) Wessler, B.; Lange, F. F.; Mader, W. *J. Mater. Res.* **2002**, *17*, 1644.

(S2) Gu, S. L.; Zhang, R.; Sun, J. X.; Zhang, L.; Kuech, T. F. *Appl. Phys. Lett.* **2000**, *76*, 3454.

(S3) Lee, Y. J.; Sounart, T. L.; Liu, J.; Spoerke, E. D.; McKenzie, B. B.; Hsu, J. W. P.; Voigt, J. A. *Cryst. Growth Des.* **2008**, *8*, 2036.